Arch. Metall. Mater. **71** (2026), 1, 269-276

DOI: https://doi.org/10.24425/amm.2026.157788

D. KUC[1*], M. SOZAŃSKA[1], K. BRZYSKI[1], B. CHMIELA[1]

INFLUENCE OF HEAT TREATMENT ON THE MICROSTRUCTURAL CHANGES OF 22MnB5 STEEL WITH AN OXIDATION-RESISTANT Al-Si COATING

This study investigates the influence of heat treatment parameters during the industrial hot stamping process on the microstructure and phase composition of Al-Si coatings applied to 22MnB5 steel. The Al-Si coating effectively protects the steel substrate against high-temperature oxidation and reduces the risk of stress-corrosion cracking. Extended austenitization promoted Fe-Al interdiffusion and phase transformations at the coating-substrate interface. Prolonged dwell times facilitated the formation of more ductile FeAl intermetallic phases, although the number of Kirkendall voids also increased. At the same time, austenite grain growth was observed in the substrate, which may adversely affect the mechanical properties of the steel.

Keywords: 22MnB5 steel; coating; hot stamping; diffusion layer; corrosion resistance; microstructure

1. Introduction

Steels used for automotive body components are often subjected to the hot stamping process, which allows the production of high-strength parts with tensile strength exceeding 1500 MPa. Such materials are commonly referred to as press-hardening steels (PHS), with typical examples being 22MnB5 and 38MnB5 grades containing increased boron content [1-3]. A key issue for 22MnB5 steel used in hot stamping is its resistance to oxidation and corrosion under high-temperature conditions as well as during service.

Al-Si coatings provide effective protection against oxidation and decarburization during austenitization by forming intermetallic layers and a continuous Al_2O_3 film [4,5]. At the same time, they reduce the susceptibility of stamped components to stress-corrosion cracking and hydrogen embrittlement, which is a significant advantage over other coating systems such as zinc-based ones [6,7].

The hot stamping process produces components of increased safety and high strength, which results from the martensitic microstructure formed during rapid cooling in the water-cooled steel die after plastic deformation under the press. A schematic diagram of a typical industrial hot stamping line is shown in Fig. 1. The quenching process requires austenitization of the steel sheets before forming at temperatures of 900°C or higher. Previous studies have indicated that austenitization at this temperature ensures a favorable balance between strength and ductility [5].

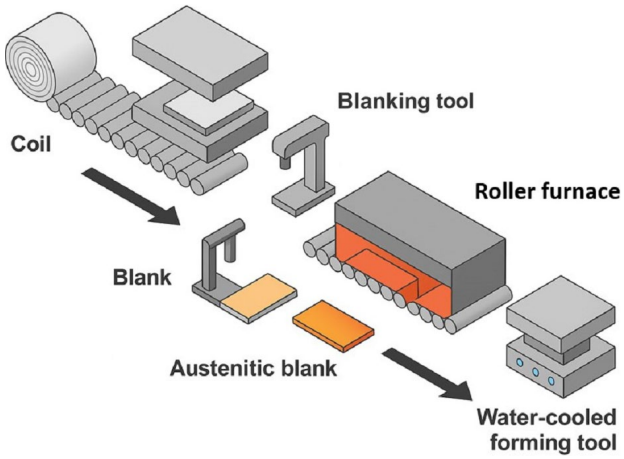

Fig. 1. Schematic diagram of an industrial hot stamping line (adapted from [1])

In the commonly used production lines equipped with continuous furnaces without protective atmospheres, coated sheets are necessary to prevent high-temperature oxidation of the steel surface during heating. Although the heat treatment

[1] SILESIAN UNIVERSITY OF TECHNOLOGY, FACULTY OF MATERIALS ENGINEERING AND INDUSTRIAL DIGITALIZATION, DEPARTMENT OF MATERIALS TECHNOLOGY, 8 KRASIŃSKIEGO STR., 40-019 KATOWICE, POLAND

* Corresponding author:dariusz.kuc@polsl.pl

time is usually short (5-10 min), oxidation and decarburization of uncoated steel can significantly reduce the mechanical strength of thin-walled components (1-2 mm). Moreover, the corrosion-resistant coating also improves the durability of the final products during service.

In industrial practice, the coatings are mainly AlSi10 layers deposited by hot dipping. The use of zinc-based coatings is not possible because of the low boiling point of zinc [7]. The parameters of the austenitization process must ensure the formation of a fully homogeneous austenitic structure, which in turn leads to the desired martensitic structure after rapid cooling in the press.

During heating, phase evolution occurs within the coating due to intensive diffusion of iron, aluminum, and silicon [8,9]. The formation of Fe-Al and Fe-Al-Si intermetallic phases ensures adequate high-temperature corrosion resistance. A properly developed intermetallic layer provides durable oxidation resistance, eliminating the need for phosphating before applying paint coatings to the final parts after hot stamping.

During austenitization, heat-resistant intermetallic phases are formed in the binary Fe-Al and ternary Fe-Al-Si systems, with varying stoichiometry depending on process parameters [9]. According to literature data, diffusion of Fe, Al and Si begins at temperatures above 600°C [10]. Therefore, selecting appropriate austenitization parameters, particularly the soaking time, is essential not only for the final mechanical properties of the steel but also for the resulting thickness and phase composition of the coating.

The heating rate to the austenitization temperature should be relatively low, below 10°C/s, to avoid melting and flow of the coating metal. Coatings rich in brittle, aluminum-based phases may crack during forming. Conversely, Fe-rich phases, such as FeAl, are more ductile and improve weldability of stamped components; thus, the outer layer of the coating should contain a higher iron content [10].

The main objective of this study was to analyze the effect of soaking time (300 s and 700 s) during heat treatment on an industrial hot stamping line on the thickness and phase composition of AlSi10 coatings. The treatment temperature was determined by the technological constraints of the production line and the process requirements and remained constant throughout the experiment.

The results are important for the optimization of industrial processes in the automotive sector, enabling the production of components with the required mechanical properties while reducing manufacturing costs and minimizing the number of defective products that may result from technological errors, such as excessive soaking time in the furnace.

2. Experimental Procedure

The material investigated was 22MnB5 steel containing 0.22%C, 1.2%Mn, 0.2%Si, 0.25%Cr and 0.004%B (wt.%), after cold rolling and subsequent application of an Al with 10% Si (AlSi10) coating at 675°C. Prior to hot stamping, the steel sheets were austenitized in a continuous roller furnace designed for industrial-scale heat treatment.

The furnace consisted of five heating zones with temperatures of 600, 650, 700, 800 and a final temperature of 910°C. The temperature on the sheet surface was measured using thermocouples. The residence times of the sheets in the furnace were 300 s and 700 s, corresponding to austenitization times of approximately 220 s and 460 s, respectively. Based on previous dilatometric studies, the Ac_3 temperature of the examined steel was determined to be 835°C. This temperature was reached after 80 s and 240 s of soaking within the furnace for the respective treatment durations.

The microstructure and coating thickness were examined using an Olympus GX71 light microscope (LM) in bright-field mode on both the surface and cross-sections of the samples taken along the rolling direction, for the initial condition and after heat treatment.

Microstructural observations and chemical composition analyses were performed using a Hitachi 3400N scanning electron microscope (SEM) equipped with a Thermo NORAN energy-dispersive X-ray spectrometer (EDS) and a System SEVEN microanalysis system. Imaging was carried out using a backscattered electron (BSE) detector under low vacuum conditions (70 Pa chamber pressure) with an accelerating voltage of 15 keV. The chemical composition was determined by EDS in selected areas.

Static tensile tests were conducted on a Zwick/Roell testing machine, and hardness was measured using the Vickers method (HV10) on a Zwick 3212002/00 hardness tester.

3. Results and Discussion

3.1. Microstructure of 22MnB5 steel with AlSi10 coating (LM observations)

The microstructures of 22MnB5 steel with an AlSi10 coating, observed on longitudinal cross-sections in the initial condition and after hot stamping, are presented in Fig. 2. After the process, the steel transformed from a ferritic (F) – pearlitic (B) structure typical of annealed materials into a fully martensitic structure as a result of rapid cooling in a water-cooled steel die. Compared with the initial state (Fig. 2a), the coating thickness increased after hot stamping due to diffusion processes, with the growth being more pronounced for longer soaking times (Fig. 2b, c). The optical microscopy observations revealed that the coating has a multiphase structure, as indicated by the contrast variation between different phases.

After heat treatment, small voids were observed within the coating, while local cracks were formed due to the mechanical pressure exerted by the die during forming. The coating in the as-received state exhibited a total thickness ranging from 24.5 to 26.7 μm. Near the steel substrate, a darker diffusion layer (DL) was visible, with an average thickness of approximately 4.5 μm and local regions up to 9 μm.

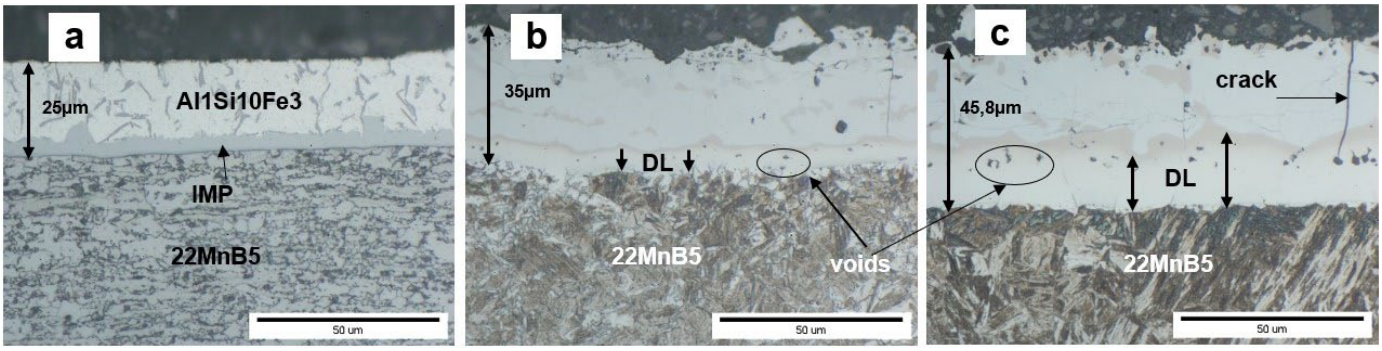

Fig. 2. Microstructure of 22MnB5 steel with AlSi10 coating on a longitudinal cross-section: (a) as-received condition; (b, c) after hot stamping with soaking times of 300 s and 700 s, respectively (LM)

After heat treatment with a soaking time of 300 s, the total coating thickness increased to 33.9-36.9 µm, and the DL reached an average thickness of about 7.3 µm. Extending the soaking time to 700 s intensified diffusion processes, resulting in a thicker DL (~19.6 µm on average) and a total coating thickness of approximately 45.8 µm.

3.2. Microstructure of 22MnB5 steel with AlSi10 coating as-received condition (SEM and EDS analysis)

In the as-received condition, after rolling and coating deposition at 675°C, the investigated 22MnB5 steel exhibited a ferritic (F) microstructure with degraded pearlite plates (P), which may indicate the beginning of upper bainite (B) formation (Fig. 3a, b). The elemental distribution within the outer coating layer was non-uniform, as confirmed by linear and area EDS concentration profiles (Figs. 3 and 4).

The coating consisted mainly of an aluminum-rich matrix with silicon segregations formed during the eutectic transformation upon cooling after coating deposition (Fig. 4, TABLE 1 – regions 1 and 2). Elongated Si-rich phases were visible, while only minor amounts of iron were detected in this layer (Fig. 4).

In the inner layer, located closer to the steel substrate and characterized by a brighter contrast in SEM images (marked as IMP in Fig. 4c), an increased iron concentration was observed

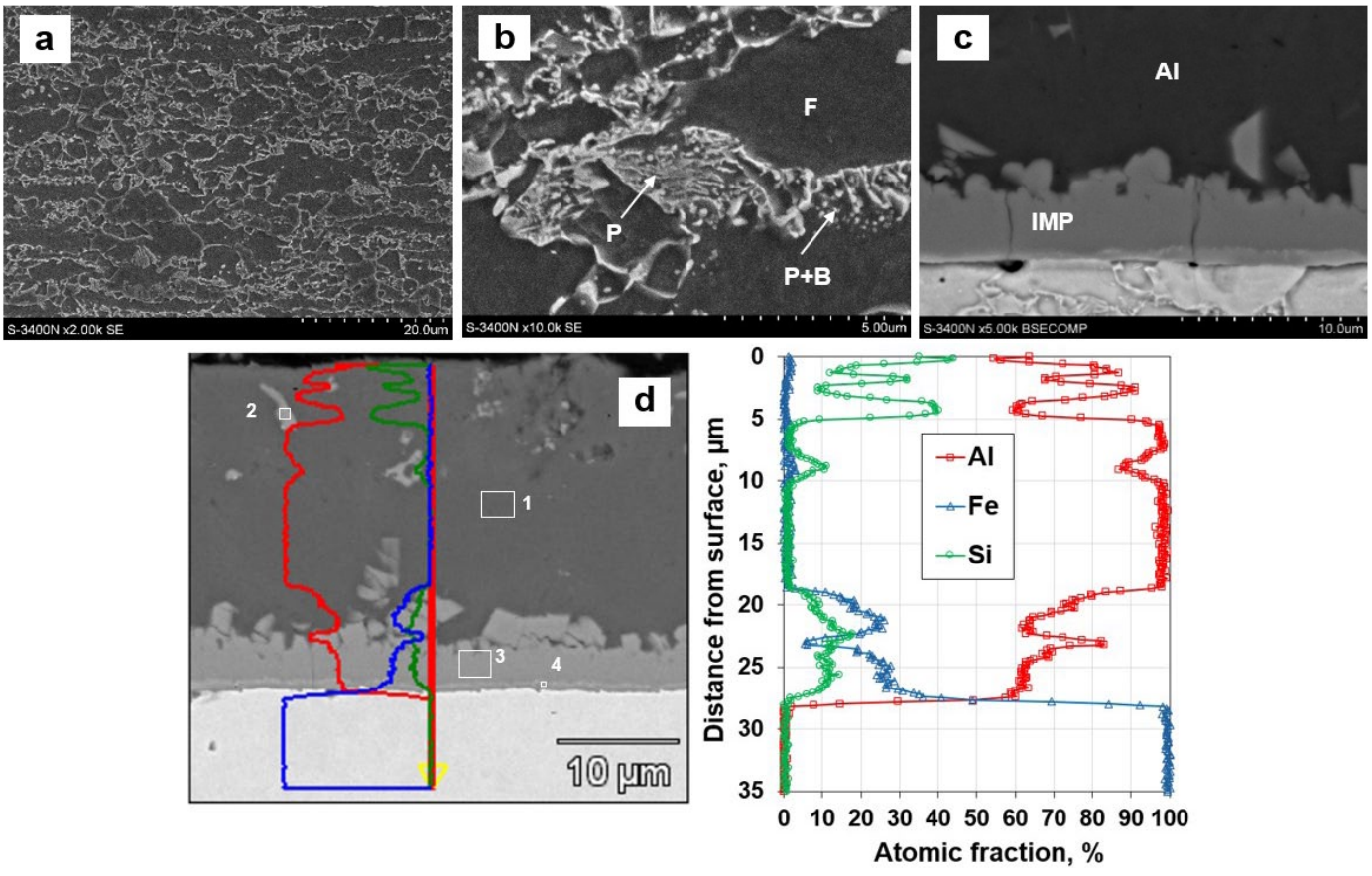

Fig. 3. Microstructure of 22MnB5 steel with AlSi10 coating in the as-received condition before hot stamping, (SEM – a, b, c; EDS line profiles – d)

(Fig. 4d). The data summarized in Fig. 4d and TABLE 1 suggest the presence of intermetallic phases of variable stoichiometry, generally of the $Fe_xAl_ySi_z$ type.

A very thin, bright-contrast layer was also visible at the steel-coating interface, enriched in iron (≈49.5 at.%), aluminum (≈44.5 at.%) and silicon (≈6 at.%), which corresponds to the composition of the FeAl phase containing silicon in solid solution.

TABLE 1

Chemical composition of the AlSi10 coating in the as-received condition (at.%) determined by EDS in the regions marked in Fig. 3d. Values are given as mean ± standard deviation (SD at.%)

Chemical composition, %at. / ± SD %at.	Al-K	Si-K	Fe-K
p. 1	98.9 ± 0.8	1.1± 0.2	—
p. 2	88.7 ± 0.7	11.2 ± 0.4	—
p. 3	63.3 ± 0.5	10.8 ± 0.4	25.9 ± 0.8
p. 4	58.0 ± 0.5	6.0 ± 0.4	36.0 ± 0.8

3.3. Microstructure of 22MnB5 steel with AlSi10 coating after heat treatment for 300 s (SEM and EDS analysis)

The microstructure of 22MnB5 steel samples with the AlSi10 coating after hot stamping with a soaking time of 300 s, as well as the corresponding linear EDS concentration profiles, are presented in Fig. 5. After the process, the steel exhibited a predominantly martensitic microstructure with small regions of upper bainite (upper-B) and locally with morphologies indicating the presence of lower bainite (lower-B) (Fig. 5a, b).

The coating microstructure changed significantly compared with the as-received state due to element diffusion processes (Fig. 5c). The distribution of aluminum, silicon, and iron became non-uniform, as shown by the EDS elemental maps (Fig. 6). Because of its low concentration, manganese diffusion was not analyzed.

Iron diffusion towards the coating surface resulted in an increased Fe concentration in the outer layer, which in the as-received condition consisted mainly of aluminum and silicon. In the middle region of the coating, a relatively homogeneous concentration of elements was observed. For example, in region 1, the average chemical composition was: Al – 57.6 at.%, Fe – 38.7 at.% and Si – 3.7 at.% (Fig. 5d, TABLE 2). This composition corresponds to an intermetallic phase of the Al_5Fe_2 type containing silicon in solid solution, consistent with previous reports [5]. Some authors also indicate the possible presence of $FeAl_2$ phase [9].

Additionally, elongated bright-contrast regions were identified (Fig. 5d, TABLE 2, regions 2 and 3), containing approximately Fe – 43.2 at.% Al – 41.5 at.% and Si – 19.3 at.%, which correspond to the FeAl phase with silicon dissolved in solid solution (up to 16% [2]).

TABLE 2

Chemical composition of the coating after hot stamping with a soaking time of 300 s (at. %) determined by EDS in the regions marked in Fig. 5d. Values are given as mean ± standard deviation (SD at.%)

Chemical composition, %at. / ± SD %at.	Al-K	Si-K	Fe-K
p. 1	57.6 ± 0.8	3.7 ± 0.2	38.7 ± 0.5
p. 2	33.5 ± 0.6	19.3 ± 0.4	46.8 ± 0.8
p. 3	33.2 ± 0.5	13.0 ± 0.4	52.2 ± 0.8
p. 4	43.6 ± 0.8	12.2 ± 0.3	44.2 ± 0.5
p. 5	15.2 ± 0.4	2.1 ± 0.3	84.8 ± 0.8

Diffusion of aluminium and silicon towards the steel substrate resulted in an increase in the thickness of the DL compared with the as-received condition. Due to differences in diffusion rates of aluminum and iron, Kirkendall voids were observed within the DL (Fig. 6c) [10,11].

The chemical composition of this DL gradually changed, with decreasing aluminium and silicon contents towards the steel

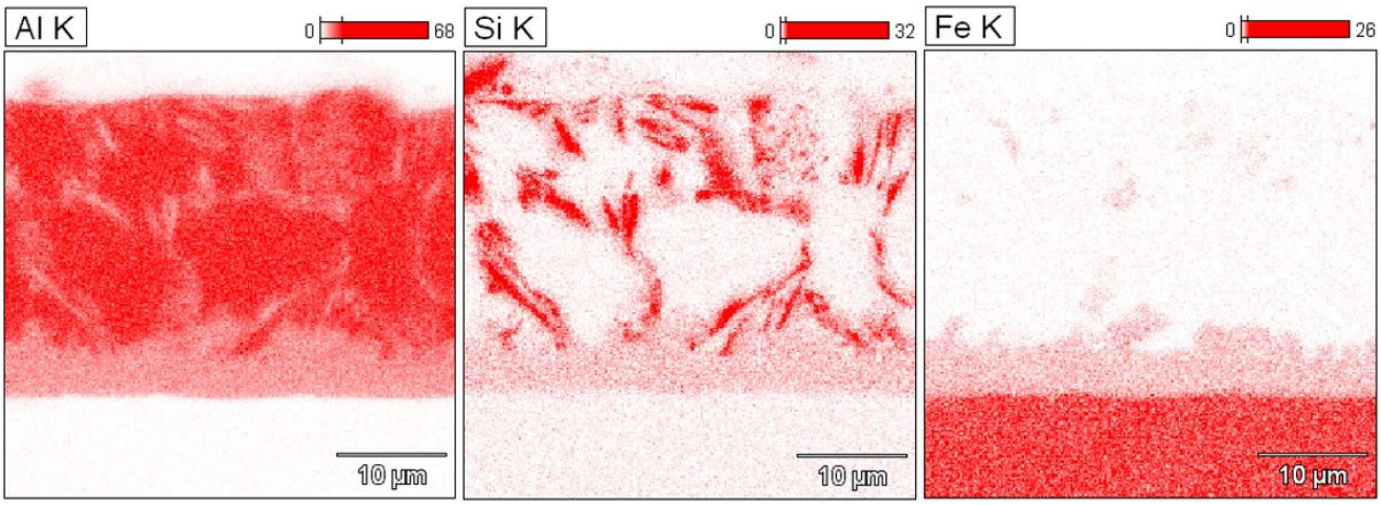

Fig. 4. Elemental concentration profiles (Al, Si, Fe) across the longitudinal cross-section of the coating and steel substrate in the as-received condition (EDS)

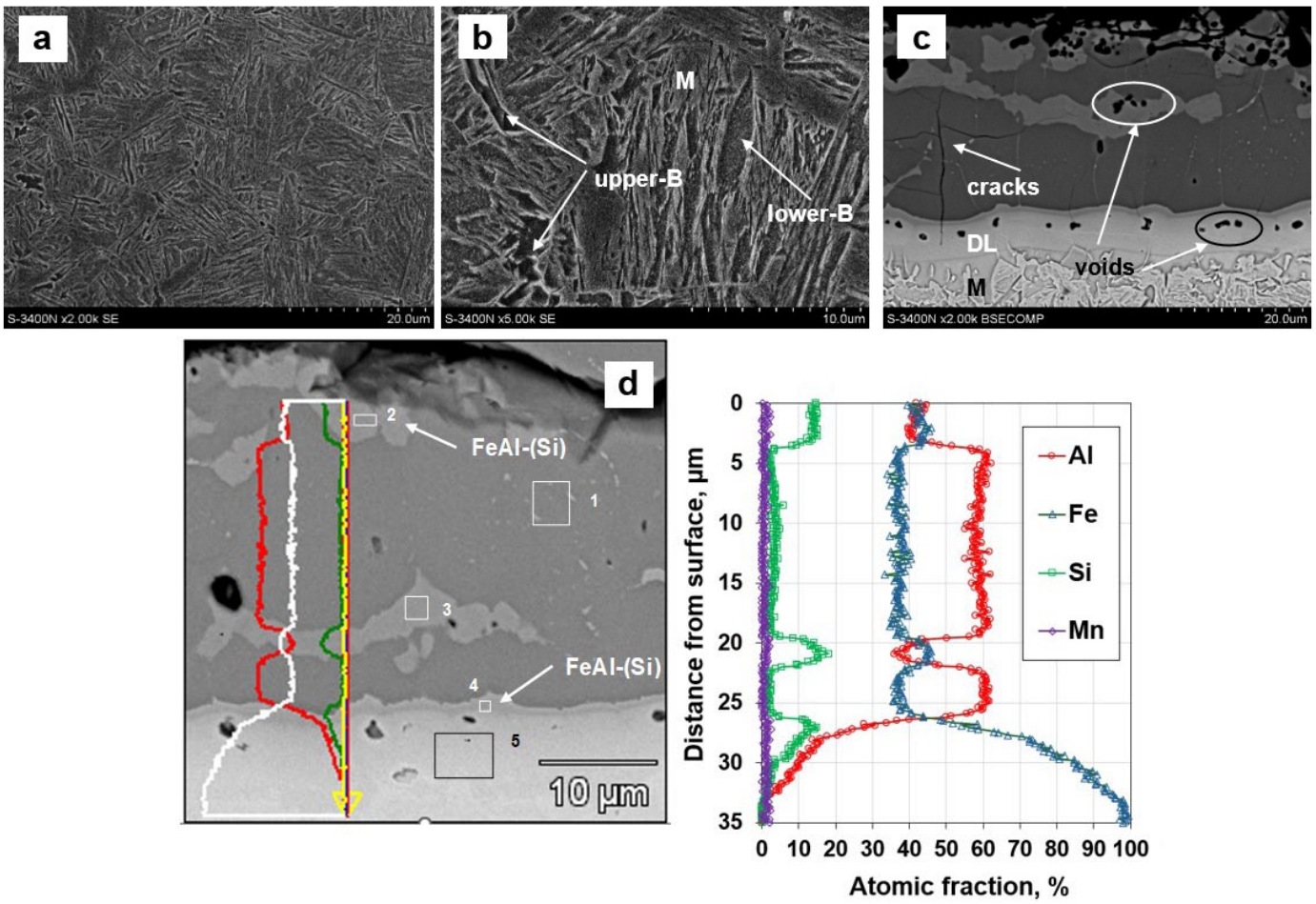

Fig. 5. Microstructure of 22MnB5 steel with AlSi10 coating after hot stamping with a soaking time of 300 s, (SEM – a, b, c; EDS line profile – d)

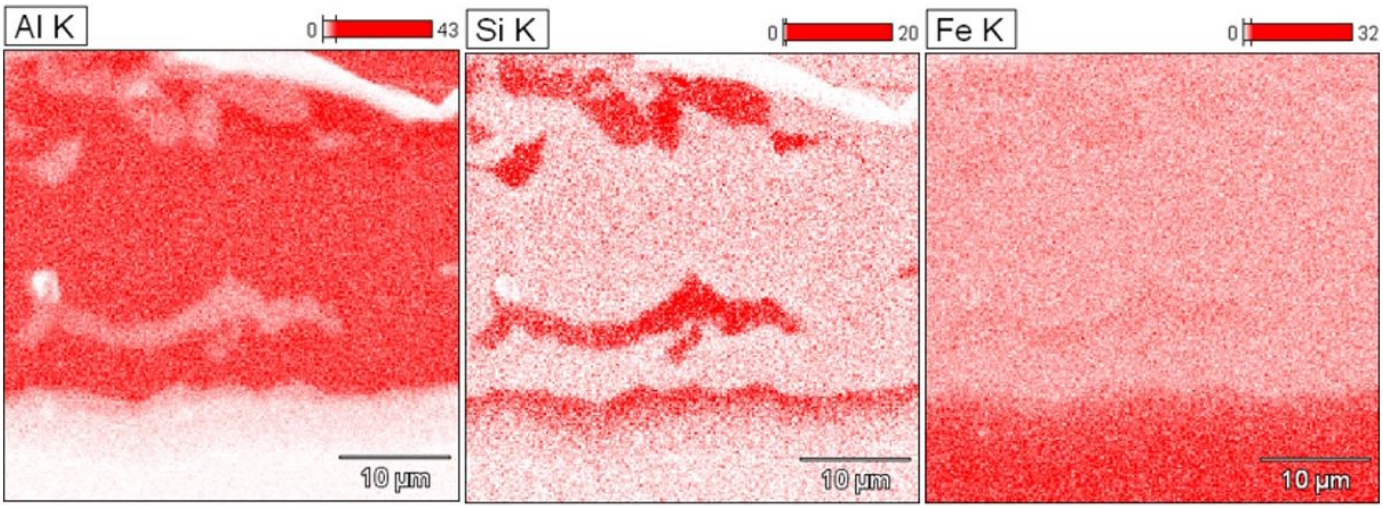

Fig. 6. Elemental concentration maps (Al, Si, Fe) across the longitudinal cross-section of the coating and steel substrate after heat treatment with a soaking time of 300 s (EDS)

substrate (Fig. 5d, TABLE 3). In the outer part of the DL, an intermetallic phase of the AlFe type (Al – 44.7 at.%, Fe – 43.1 at.%) was most likely formed, while below it a solid α-Fe solution was present, with representative compositions for regions 4 and 5 listed in TABLE 3.

3.4. Microstructure of 22MnB5 steel with AlSi10 coating after heat treatment for 700 s (SEM and EDS analysis)

The microstructure of 22MnB5 steel samples with the AlSi10 coating after hot stamping with a soaking time of 700 s, together with the corresponding EDS linear concentration pro-

files, is shown in Fig. 7. After hot stamping, the steel exhibited a fully martensitic structure with regions of different morphologies. Similar to the specimens heat-treated for 300 s, local areas indicative of lower bainite (lower-B) were observed (Fig. 7a, b).

Prolonged soaking during heat treatment resulted in a pronounced increase in the thickness of the DL. The frequency and size of Kirkendall voids also increased noticeably (Fig. 7c). In the outer coating layer, irregular bright-contrast regions were visible on SEM images, enriched in iron up to approximately 60 at.%, indicating advanced diffusion of this element towards the surface (Fig. 7d, regions 1 and 2; TABLE 3).

Similar to the heat-treated coating for 300 s, a mixed-phase region was identified, composed mainly of the intermetallic Al_5Fe_2 phase with a small fraction of FeAl (Fig. 7d, TABLE 3, region 3). Within the thick DL, distinct grain boundaries between intermetallic phases could be observed (Fig. 7c).

The chemical composition of the DL towards the steel substrate changed similarly to that in the 300 s variant, with decreasing aluminium and silicon contents in the direction of the base metal (Fig. 7d). In the outer part of the DL, an intermetallic phase of the FeAl type was most likely formed, with an average composition of Fe – 46.9 at.%, Al – 41.7 at.% and Si – 11.4 at.% (TABLE 3, region 4). Below this layer, a solid α-Fe solution with gradually decreasing aluminium content was observed, in accordance with the Fe-Al equilibrium system, as shown for regions 5 and 6 (TABLE 3).

TABLE 3

Chemical composition (at. %) of the coating after hot stamping with a soaking time of 700 s determined by EDS in the regions marked in Fig. 7d. Values are given as mean ± standard deviation (SD at.%)

Chemical composition, %at. / ± SD %at.	Al-K	Si-K	Fe-K
p. 1	59.3 ± 0.5	1.3 ± 0.1	39.4 ± 0.6
p. 2	33.1 ± 0.6	10.0 ± 0.2	55.8 ± 0.8
p. 3	33.4 ± 0.6	8.1 ± 0.2	57.1 ± 0.8
p. 4	41.7 ± 0.8	11.4 ± 0.3	46.9 ± 0.7
p. 5	15.4 ± 0.3	4.6 ± 0.2	80.0 ± 0.8
p. 6	5.7 ± 0.2	1.1 ± 0.2	93.2 ± 0.8

3.5. Mechanical properties of 22MnB5 steel

The mechanical properties of 22MnB5 steel in the as-received condition and after hot stamping are summarized in TABLE 4. After the process, a significant increase in both hardness (by approximately 1.7 times) and tensile strength (more than twice) was observed because of the martensitic transformation during rapid cooling in the steel die. At the same time, elongation decreased by more than twofold compared with the as-received state.

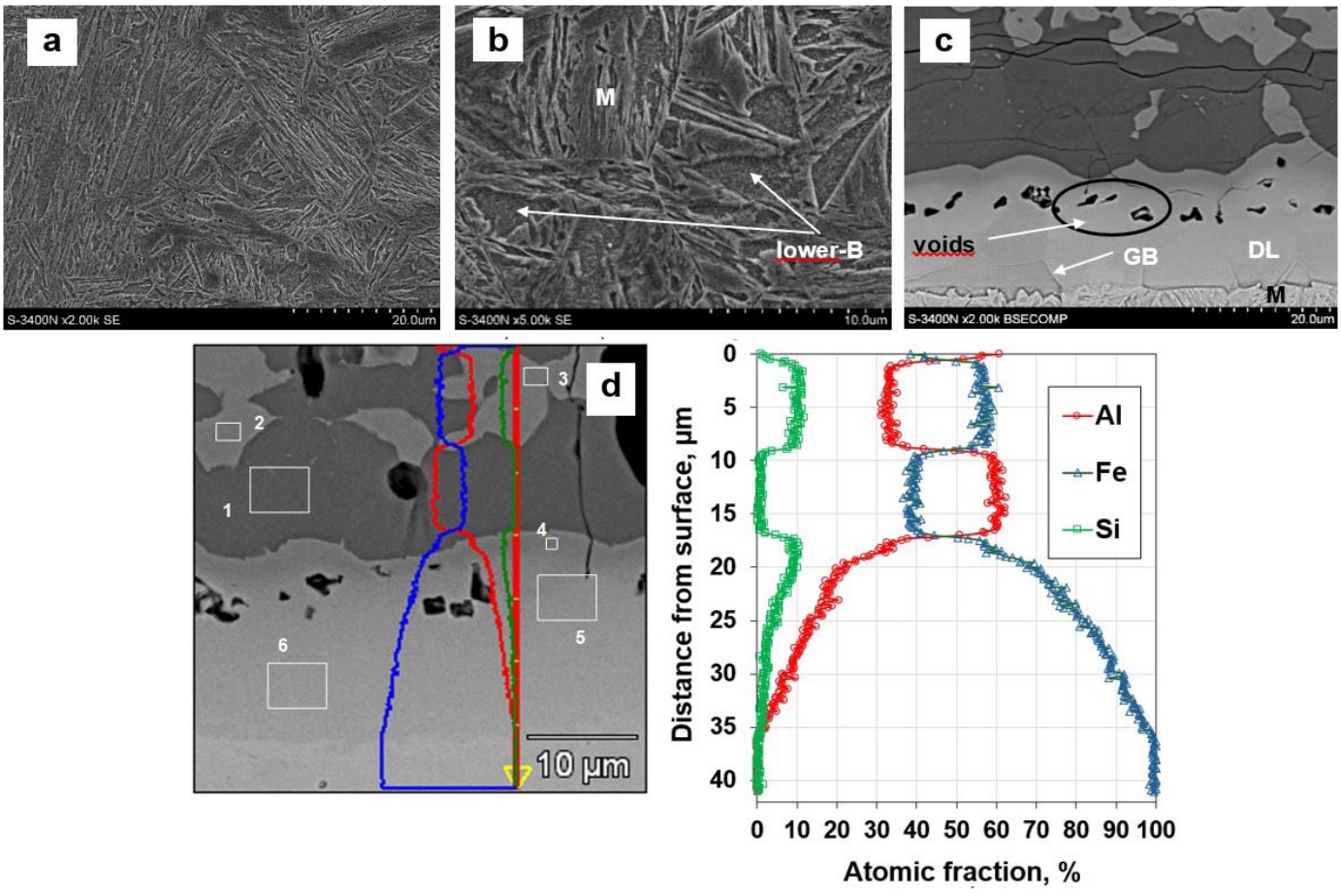

Fig. 7. Microstructure of 22MnB5 steel with AlSi10 coating after hot stamping with a soaking time of 700 s, (SEM – a, b, c; EDS line profile – d)

TABLE 4

Mechanical properties of 22MnB5 steel in the as-received condition and after hot stamping with different soaking times, N = 10 for hardness measurements, N = 3 for tensile tests

Condition	Hardness HV10	Tensile test			Number of replicates (N)
		Yield strength, $R_{p0,2}$, MPa	Tensile strength R_m, MPa	Elongation A_{50}, %	
As-received, coated	260 ± 5	399 ± 10	596 ± 15	20,5± 3	10 (Hardness) / 3 (Tensile)
Required after hot stamping	*400-510*	*950-1250*	*1300-1650*	*>5*	—
Soaking – 300 s	450 ± 7	1210 ± 20	1430 ± 25	7,3 ± 2	10 / 3
Soaking – 700 s	455 ± 6	1180 ± 15	1450 ± 20	7,1 ± 3	/ 3

No distinct influence of the soaking time on the mechanical properties was identified. The measured hardness (HV10), yield strength ($R_{p0.2}$), tensile strength (R_m) and total elongation (A_{50}) values were within the range required for hot-stamped parts.

4. Summary and conclusions

Al-Si coatings applied to 22MnB5 steel intended for hot stamping serve a dual purpose: they protect the steel against oxidation and decarburization during austenitization and improve corrosion resistance under service conditions. Intermetallic layers formed during heating (mainly Fe_2Al_5, FeAl, and to a lesser extent $FeAl_2$ and ternary Fe-Al-Si phases) act as diffusion barriers, limiting oxygen transport into the steel substrate [6,8]. Above 600°C, a continuous Al_2O_3 layer forms on the surface, stabilized by silicon, which further enhances resistance to high-temperature oxidation [5].

In humid service environments, stress-corrosion cracking induced by hydrogen represents a major risk. During hot stamping and austenitization, water vapour may react with aluminum, producing atomic hydrogen. Hydrogen diffusion into the martensitic matrix of 22MnB5 steel increases the risk of delayed fracture [6]. This phenomenon can be mitigated by optimizing heat treatment parameters, reducing Kirkendall voids, and ensuring the formation of an Fe-rich (FeAl-type) outer coating layer, which provides higher ductility and better weldability [4,10].

In contrast to zinc coatings, which cannot be used in hot stamping due to the low boiling point of zinc (907°C), Al-Si coatings provide both oxidation protection during heating and durable atmospheric corrosion resistance in service [11,12]. Literature reports also indicate that such coatings can eliminate the need for phosphating prior to cathodic electrodeposition painting, which is advantageous for industrial practice [1].

From the industrial standpoint, the hot stamping process should be as short as possible while maintaining optimal properties. For both soaking times investigated (300 s and 700 s), a predominantly martensitic structure was obtained with some regions of lower bainite morphology. Small areas of upper bainite observed after shorter soaking (300 s) are unfavorable for service performance. The region marked as lower bainite in Fig. 5 may also include self-tempered martensite, as both microstructures are morphologically similar. According to previous studies on PHS, the relatively high M_s (~410-430°C) temperature of 22MnB5 promotes the precipitation of fine transition carbides during cooling, which is characteristic of self-tempering [3,13,14].

Mechanical testing showed that extending the austenitization time to 700 s caused a slight decrease in yield strength ($R_{p0.2}$) but a marginal increase in tensile strength (R_m). This behavior results from grain growth of austenite during prolonged soaking, which slightly reduces yield strength, while improved austenite homogeneity enhances tensile strength. No reduction in ductility was observed with increasing soaking time.

The coating structure evolved during heat treatment due to diffusion of aluminum, silicon and iron, forming several intermetallic phases with variable compositions. Prolonged soaking increased both the total coating thickness and the DL thickness. A higher iron concentration in the surface region promoted the formation of the more ductile FeAl phase, while reducing the fraction of brittle Fe_2Al_5 and $FeAl_2$ phases, thus minimizing cracking during forming. However, the number and size of Kirkendall voids increased with longer soaking times.

To fully determine the phase composition of the coating, further studies using electron backscatter diffraction (EBSD) are recommended. Additionally, analysis of diffusion kinetics, diffusion coefficients, and diffusivity would enable the development of a physical model describing coating structure evolution under hot stamping heat treatment conditions.

Acknowledgements

This research was carried out at the Silesian University of Technology, Faculty of Materials Engineering and Industrial Digitalization, Department of Materials Technology, and was co-funded under the programme of the Polish Ministry of Science and Higher Education "Doktorat wdrożeniowy".

REFERENCES

[1] T. Taylor, A. Clough, Critical review of automotive hot-stamped sheet steel from an industrial perspective. Mater. Sci. Technol. **34** (10), 809-861 (2018). DOI: https://doi.org/10.1080/02670836.2018.1425239

[2] I. Wróbel, A. Skowronek, A. Grajcar, A review on hot stamping of advanced high-strength steels: Technological-metallurgical aspects and numerical simulation. Symmetry **14**, 1-17 (2022). DOI: https://doi.org/10.3390/sym14010017

[3] H. Karbasian, A.E. Tekkaya, A review on hot stamping. J. Mater. Process. Technol. **210**, 2103-2118 (2010).
DOI: https://doi.org/10.1016/j.jmatprotec.2010.07.019

[4] D. Schwingel, H. Karbasian, M. Merklein (Eds.), Hot Stamping of Ultra High-Strength Steels. Springer International Publishing, Cham, **394** (2018).
DOI: https://doi.org/10.1007/978-3-319-98870-2

[5] M. Windmann, A. Röttger, W. Theisen, Formation of intermetallic phases in Al-Si coating on 22MnB5 steel during hot stamping. Surf. Coat. Technol. **246**, 17-25 (2014).
DOI: https://doi.org/10.1016/j.surfcoat.2014.02.056

[6] W. Yang, E. Hwang, H. Kim, S. Ahn, S. Kim, H. Castaneda, A study of annealing time to surface characteristics and hydrogen embrittlement on Al-Si coated 22MnB5 during hot stamping process. Surf. Coat. Technol. **378**, 124911 (2019).
DOI: https://doi.org/10.1016/j.surfcoat.2019.124911

[7] L. Dosdat, J. Petitjean, T. Vietoris, O. Clauzeau, Corrosion resistance of different metallic coatings on press-hardened steels for automotive. Steel Res. Int. **82**, 726-733 (2011).
DOI: https://doi.org/10.1002/srin.201000291

[8] L. Cho, L. Golem, E.J. Seo, D. Bhattacharya, J.G. Speer, K.O. Findley, Microstructural characteristics and mechanical properties of the Al–Si coating on press-hardened 22MnB5 steel. J. Alloys Compd. **846**, 156349 (2020).
DOI: https://doi.org/10.1016/j.jallcom.2020.156349

[9] D.W. Fan, H.S. Kim, J.K. Oh, K.G. Chin, B.C. De Cooman, Coating degradation in hot press forming. ISIJ Int. **50**, 561-568 (2010).
DOI: https://doi.org/10.2355/isijinternational.50.561

[10] D.W. Fan, B.C. De Cooman, Formation of an aluminide coating on hot-stamped steel. ISIJ Int. **50**, 1713-1718 (2010).
DOI: https://doi.org/10.2355/isijinternational.50.1713

[11] P. Novák, A. Michalcová, I. Marek, On the formation of intermetallics in the Fe–Al system: An in situ XRD study. Intermetallics **32**, 127–136 (2013).
DOI: https://doi.org/10.1016/j.intermet.2012.08.020

[12] L. Cho, L. Golem, E.J. Seo, D. Bhattacharya, J.G. Speer, K.O. Findley, Microstructural characteristics and mechanical properties of the Al–Si coating on press-hardened 22MnB5 steel. J. Alloys Compd. **846**, 156349 (2020).
DOI: https://doi.org/10.1016/j.jallcom.2020.156349

[13] Y. Zhang, W. Hui, X. Zhao, C. Wang, H. Dong, Effects of hot stamping and tempering on hydrogen embrittlement of a low-carbon boron-alloyed steel. Materials **11** (12), 2507 (2018).
DOI: https://doi.org/10.3390/ma11122507

[14] R. Esterl, M. Sonnleitner, M. Stadler, G. Wölger, R. Schnitzer, Microstructural characterization of ultra-high strength martensitic steels. Pract. Metallogr. **55** (4), 203-222 (2018).
DOI: https://doi.org/10.3139/147.110491